Tc-99m-sestamibi/Tc-99m-pertechnetate dual-tracer scintigraphy of parathyroid glands with double image subtraction: A dedicated short execution time protocol

Objective: Parathyroid scintigraphy is one of the most common imaging techniques utilized for preoperative detection of hyper-functioning parathyroid glands. Since 1980, numerous scintigraphic protocols have been used with no established uniform technique. Majority of these techniques expressed by the gamma camera occupation time and the patient presence time in the nuclear medicine facilities last at least 3 to 4 hours. We describe an in-house short execution time scintigraphic protocol, lasting 1 hour and using dual-tracer with double image subtraction.

Methods: Our in-house protocol is based on the acquisition of multiple images view of the cervical and mediastinal regions, after successive intravenous injections of Tc-99m-sestamibi and Tc-99m-pertechnetate to detect and localize either orthotopic or ectopic hyper functioning parathyroid glands. Double subtraction of thyroid region images allows visualization of parathyroid lesions. Six representative positive cases of our protocol were selected among 286 cases enrolled between January 2017 and December 2019 with clinically and biologically documented hyperparathyroidism and being candidates for surgery.

Results: In 5 cases of primary and 1 case of secondary hyperparathyroidism, there was a tendency of linear correlation between the activity level of the true positive foci, the size of gland documented by histology, and the serum levels of parathyroid hormone and calcium. The false-positive foci of activity revealed by our protocol are related to motion artifact or concomitance of a multi-nodular thyroid goiter.

Conclusion: According to an extensive comparative review of the literature data, the main technical particularities of our challenging protocol lie in its promising performance, short execution time, and low cost.

KEYWORDS: hyperparathyroidism ▪ parathyroid scintigraphy ▪ Tc-99m-sestamibi ▪ Tc-99m-pertechnetate ▪ image subtraction

Introduction

Minimally invasive parathyroidectomy is the treatment of choice of Hyper Para Thyroidism (HPT). Most surgeons tend to perform a targeted ablation of the Hyper-Functioning Parathyroid Glands (HFPG) based on reliable imaging studies that allow the selection of eligible patients and identification of ectopic glands [1, 2]. Para Thyroid Scintigraphy (PTS) is one of the most common imaging techniques utilized for the preoperative localization of HFPG [3]. PTS has become widely used as first-line diagnostic imaging in combination with Echography (ECHO). The Dynamic Computed Tomography (DCT) and Magnetic Resonance Imaging (MRI) are reserved as resolving methods in more complicated cases [4]. There is increasing interest in introducing new sensitive methodologies to localize the HFPG, as the F-18-choline positron emission tomography in combination with the computed tomography (F-18-Choline PET/CT). However, their indications in HPT require clarification alongside scintigraphy techniques that are approved and much cheaper [5]. Since the 1980s, nuclear medicine physicians have practiced numerous protocols of PTS. These protocols could be classified into two main groups, the single-tracer dual-phase scintigraphy using the Tc-99m-sestamibi (MIBI) and the dual-tracer subtraction scintigraphy using Tl-201/Tc-99m, I-131/Tl-201 or I-123/MIBI [6,7].

Feras Chehade[1]*, Ali Kanj[2], Elias Ghafari[3], Nasser Hammoud[3], Najla Fakhereddine[4], Ahmad Ghazzawi[5], Hilal Abou Zeinab[6], Khalil Jaber[6], Hassan Kazma[7] & Hamza Chehade[8]

[1]Department of Nuclear Medicine, Hammoud Hospital University Medical Center, Sidon, Lebanon

[2]Department of Radiology, Hammoud Hospital University Medical Center, Sidon, Lebanon

[3]Department of General Surgery, Hammoud Hospital University Medical

Center, Sidon, Lebanon
[4]Department of Pathology, Hammoud Hospital University Medical Center, Sidon, Lebanon
[5]Department of Endocrinology, Hammoud Hospital University Medical Center, Sidon, Lebanon
[6]Department of Nephrology, Hammoud Hospital University Medical Center, Sidon, Lebanon
[7]Department of Laboratory Medicine, Hammoud Hospital University Medical Center, Sidon, Lebanon
[8]Department of General Medicine, Hammoud Hospital University Medical Center, Sidon, Lebanon
*Author for correspondence
feras.chehade@gmail.com

The choice between these two groups of protocols depends on several factors:

1) The kinds of available radiopharmaceuticals and their associated costs [8].
2) The technical characteristics of the gamma camera, including its equipment with a pinhole collimator and capability to carry out Single-Photon Emission Computed Tomography (SPECT) in combination with Computed Tomography (CT).
3) the managing manner of the Patient Presence Time (ppT) in the nuclear medicine facility as well as the Gamma camera Occupation Time (goT), especially that majority of protocols last around 3 to 4 hours.

Our study presents the concept of an in-house Dual-tracer Double image Subtractions (DDS) protocol of parathyroid scintigraphy that we developed at Hammoud Hospital University Medical Center, Sidon, Lebanon [9]. The protocol was designed based on two main ideas, a short execution time and a low cost, which are valuable factors for the public health systems with a modest economy. The two radiotracers required in our protocol are the MIBI and the Tc-99m-pertechnetate (Tc-99m), which are both traceable with a radioisotope available daily in any nuclear medicine facility fitted with a gamma camera. Based on a review of the literature, we discuss the technical strengths and limitations of our protocol as compared to the most adopted ones on a worldwide scale.

Materials and methods

▪ Our dedicated dual-tracer double image subtractions

Our DDS protocol includes two steps of digital subtraction of thyroid region images that allow visualization of HFPG. These steps require two successive intravenous injections of the MIBI that is taken up by both the HFPG and the normal thyroid parenchyma and the Tc-99m that is taken up only by the thyroid parenchyma.

Concept of images acquisition: Initially, through a 3-way cannula, the patient received an intravenous injection of 10 MBq/Kg of MIBI. Five minutes after the injection, the patient went into a supine position on the gamma camera table (GE BRIVO) with the extension of the neck. A large field anterior view of the neck/mediastinum (covering from the parotid glands to the heart) was acquired during 5 min using a low energy high-resolution parallel holes collimator. Then, a 5 mm diameter pinhole collimator was mounted, and 5 min images of the thyroid region under both left and right lateral views were recorded. After that, the patient was instructed not to move the head/neck, acquiring an anterior view of the thyroid region during 10 min. With the gamma camera pinhole head and the patient head/neck remaining in fixed positions, a 3MBq/Kg of Tc-99m, the second radiopharmaceutical, was in stride injected through the 3-way cannula. After 10min, both tracers being simultaneously distributed along the cervical region, a 10 min (MIBI&Tc-99m) image of the thyroid region was acquired. These images were serially acquired using energy window limits of 140 KeV ± 15%. When the anterior planar view of the neck/mediastinum highlighted a focus of activity in an ectopic position, a supplement anatomical localization was carried out later through enhanced CT. The following scheme **(FIGURE 1)** illustrates the chronology of our protocol, including the 2 radiotracer injections and the serial 5 images acquisition, as shown in **FIGURE 2**.

Concept of images processing: A Region of

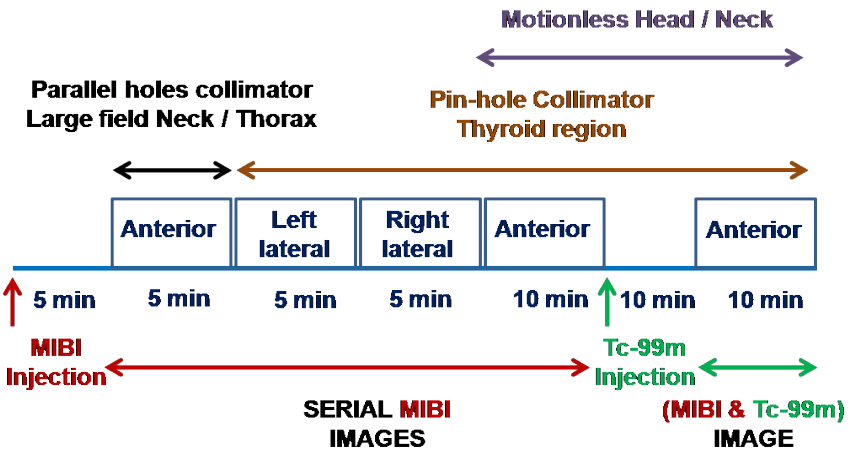

FIGURE 1. Scheme illustrating the chronology of our protocol, including the 2 radiotracer injections and the serial 5 images acquisition.

Interest (ROI) drawn around the thyroid gland of the anterior MIBI image (**FIGURE 2D**), then copied and projected on the anterior (MIBI&Tc-99m) image **(FIGURE 2E)** aims at two goals: 1) to verify the motionless of head/neck during the successive acquisition of these two images; 2) to adequately normalize images before subtraction. It is important to note that movement of the head/neck occurring during these two successive images often induces an artifact in the resultant image of subtraction. **FIGURE 3** illustrates the concept of the double image subtractions, which are basically performed by following the below two steps:

The first subtraction of the MIBI image from (MIBI&Tc-99m) image, which is acquired in an equal pre-time of 10 min, allows generating the TC thyroid gland image. This step of calculation considers that MIBI activity of the thyroid is unchanged during the time-lapse of 10 min waiting for the regular distribution of Tc-99m, meanwhile injected. The (MIBI&Tc-99m) image could be mathematically expressed in term of total counts as (MIBI+TC):

(MIBI+TC)–MIBI=TC

a) The second subtraction of the generated TC image from the MIBI image allowed the deduction of the HFPG image. MIBI image is normalized to the generated TC image after multiplication by a correction factor corresponding to the TC/MIBI ratio (na) of the average counts included in the ROI of each image.

$(n_a \times MIBI)–TC=PARATHYROID.$

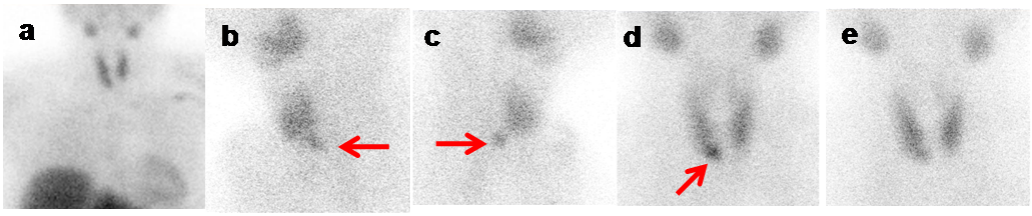

FIGURE 2. Represents the serial consecutive 5 images according to their acquisition chronology performed in a patient with primary HPT. This case highlights the importance of acquiring the left and right lateral views (b and c), which allow the in-depth visualization of HFPG that is localized just behind the right isthmo-lobar region of the thyroid gland (red arrow at images b, c and d).

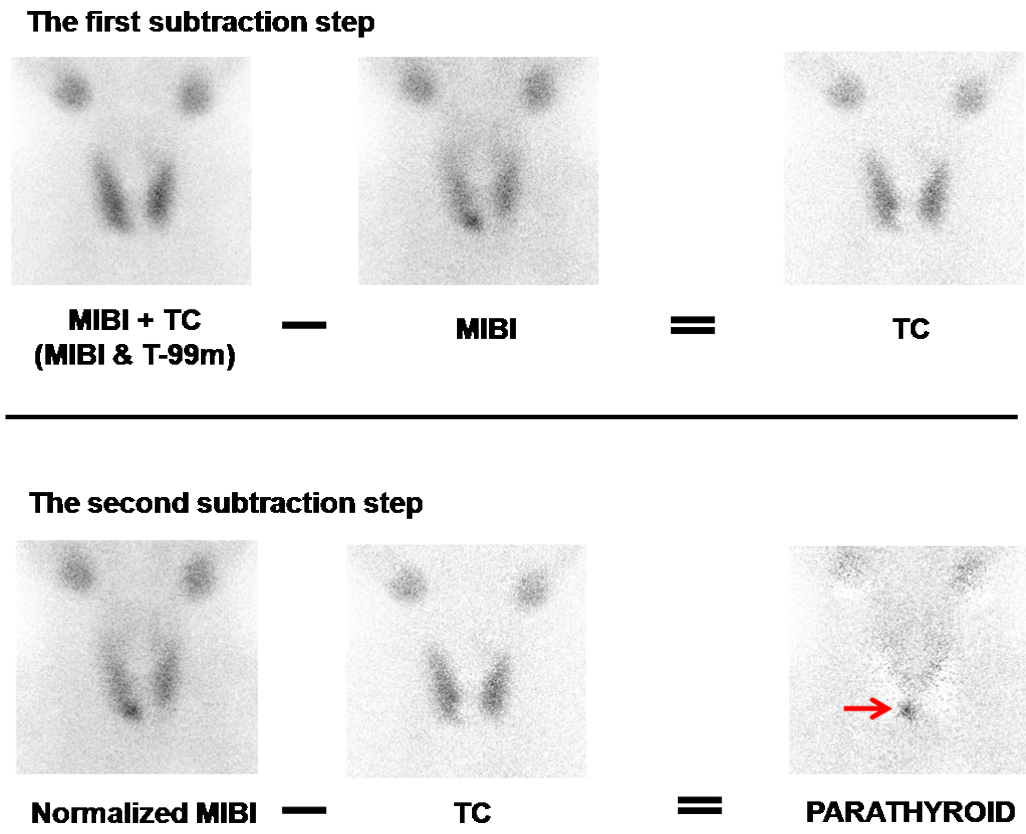

FIGURE 3. Illustrates the two subtraction steps; the first subtraction step of the MIBI image from (MIBI&Tc-99m) image generates the thyroid TC image; the second subtraction step of the TC image from the normalized MIBI image generates the HFPG image that is represented by a selective focus of tracer uptake projected along the right isthmo-lobar region (red arrow).

b) The two steps of image subtraction described above could be simplified in one step of subtraction, leading to generate the same parathyroid image **(FIGURE 4).** Indeed, the direct subtraction of (MIBI&TC) image from a normalized MIBI image leads to the exact calculation results obtained through the two steps of subtraction:

The MIBI image is normalized to the (MIBI&Tc-99m) image after multiplication by the correction factor corresponding to the (MIBI&Tc-99m)/MIBI ratio (n_b) of the average counts included in the ROI of each image. The (MIBI&Tc-99m) image could be mathematically expressed in terms of total counts as (MIBI+TC);

$n_b = (MIBI+Tc)/MIBI = 1+TC/MIBI = 1+n_a$ (since TC/MIBI=n_a as mentioned in the above paragraph of double steps of subtraction). The correction n_b factor is replaced by $(1+n_a)$ in the following equation of one step subtraction:

$(n_b \times MIBI)$-(MIBI+TC)

$(1+n_a) \times MIBI$-(MIBI+TC)

$MIBI+(n_a \times MIBI)$-MIBI-TC=$(n_a \times MIBI)$-TC=PARATHYROID, which is the same resultant equation described above in the two steps of subtraction.

The single step of image subtraction provides the advantage to avoid pixels of negative counts that occurs within the TC thyroid image of the double steps of image subtraction. The resulting images of the two steps of image subtraction and the simplified one step are qualitatively and quantitatively equivalent.

▪ Our representative DDS cases

The scientific committee of the medical ethics of the hospital has approved to implement our in-house DDS protocol and to carry out a prospective analysis of the subsequent results. Written informed consent was obtained from all patients. In this study, aiming to illustrate the relevant results of the implemented protocol, 6 representative positive cases of the methodology

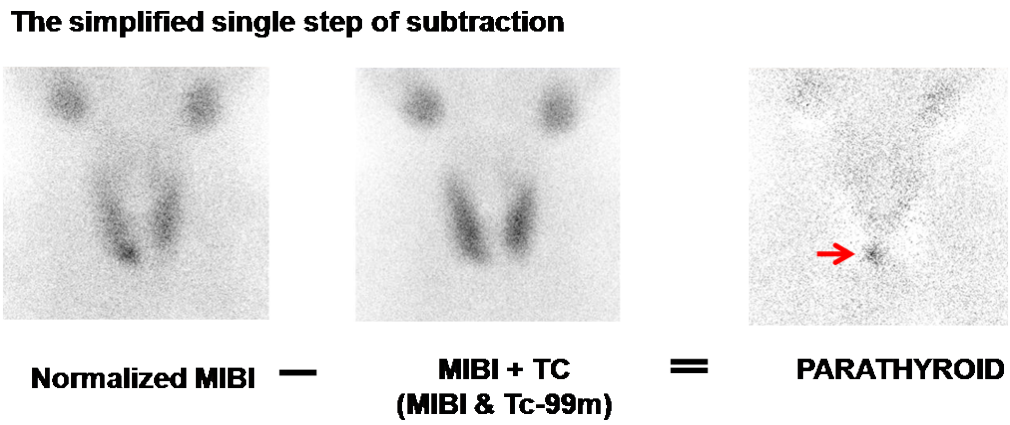

FIGURE 4. Corresponds to the simplified single-step subtraction of (MIBI&Tc-99m) image from normalized MIBI image generating the abnormal parathyroid gland image that is represented by a selective focus of tracer uptake projected along the right isthmo-lobar region (red arrow).

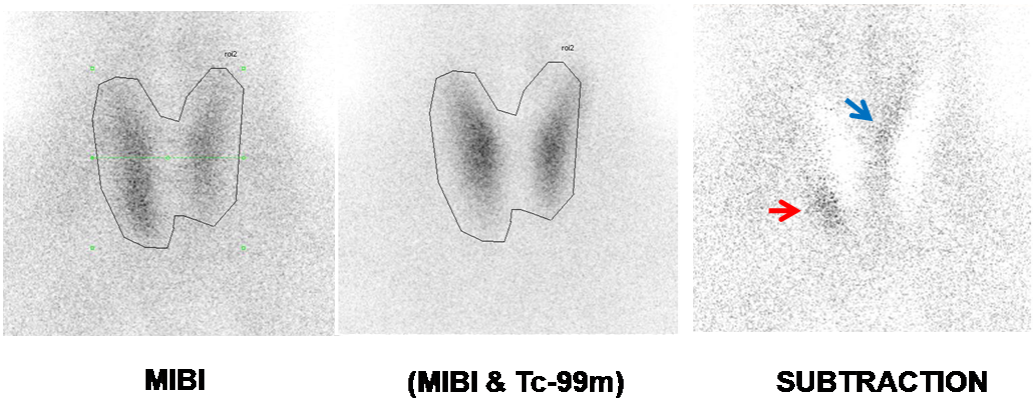

FIGURE 5. Represents the iconography of DDS performed in patient 2; the ROI drawn around the thyroid of the (MIBI) image, do not correlate with the exact topography of the gland seen on (MIBI&Tc-99m) image, a fact indicating head/neck motion during the successive acquisitions of the two images. Subtraction images show the TP focus of selective MIBI uptake projected on the lower pole of the right lobe consistent with HFPG (red arrow); the motion artifact activity revealed at the medial aspect of the left upper lobe could be easily recognized as TN (blue arrow) by comparing the pair MIBI and (MIBI&Tc-99m) images.

of DDS were selected among those performed between January 2017 and December 2019 in 286 patients with clinically and biologically documented HPT and being candidates for surgical treatment. In 5 patients the pre-surgical diagnosis of primary HPT was based on the elevated serum levels of parathyroid hormone (PTH) and calcium (Ca+), which were manifestly elevated in 4 patients (PTH=180 ng/L, 164 ng/L, 153 ng/L, and 132 ng/L; Ca+=11.5 mg/dl, 11.3 mg/dl, 10.9 mg/dl, and 11.1 mg/dl respectively) and mildly elevated in 1 patient (PTH=87 ng/L and Ca+=10.8 mg/dl). The 6th patient was uremic experiencing secondary HPT (PTH=271 ng/L and Ca+=11.9 mg/dl). None of the patients had undergone previous surgical exploration of the neck. In all patients, a supplement of ECHO documentation was performed to support the minimally invasive surgical strategy. A CT was performed in 1 patient to refine the anatomic location of an ectopic focus of MIBI uptake disclosed in the upper anterior mediastinum.

Results

▪ Findings of DDS and supplement radiological imaging

The True Positive (TP) lesions revealed by scintigraphy were visually classified as foci of high, moderate or mild activity.

1. In patient 1, a single prominent focus of selective MIBI uptake is projected behind the right isthmolobar region of the thyroid gland **(FIGURES 2-4)** and interpreted as TP lesion. This demonstrative case of our DDS protocol included 5 serial images allowing to detect the HFPG and to localize it, by mean of the lateral views, behind the right isthmolobar region.
2. DDS in patient 2 revealed 2 foci of activity in the thyroid area. The first prominent focus projected at the right lower pole is considered as a TP lesion, and the second focus generated at the upper medial aspect of the left lobe represents a motion artifact. This kind of artifact is common to any dual tracer subtraction techniques. It is easily recognized as a true negative (TN) lesion by comparing the pair MIBI and the (MIBI&Tc-99m) images **(FIGURE 5).**
3. In patient 3, a single small focus of selective MIBI uptake projected at the right lower pole of the thyroid is interpreted as a TP lesion **(FIGURE 6).** This case indicates the good sensitivity of the DDS protocol in the detection of small parathyroid adenoma (0.3 g weight according to the histological data).
4. DDS realized in patient 4 is representative of a primary HPT with a concomitant multi-hetero-nodular thyroid goiter **(FIGURE 7).** The TP hot spot of MIBI uptake projected into the left middle lobe (red arrow) consisted of an intrathyroidal parathyroid adenoma as disclosed on surgical pieces of the total thyroidectomy. The generated TC image is compatible with toxic multi-hetero-nodular goiter, revealing bilaterally at least 6 nodules, being 2 cold (green arrows), and 4 functionally active (black arrows). Thyroid nodules are a source of pitfalls occurring in the subtraction image and making tricky the scintigraphic reading by the physician. Indeed, it was difficult to discern on a subtraction image revealing several foci of activity, between the parathyroid adenoma (red arrow) and the thyroid nodules (blue arrows). The ROI drawn for the parathyroid adenoma located in the left lobe is projected in a cold area in the TC image. Thus, the parathyroid adenoma retains the MIBI only (TP lesion) and presents a different behavior compared to the small functional thyroid nodules which retain the 2 tracers (TN lesions).

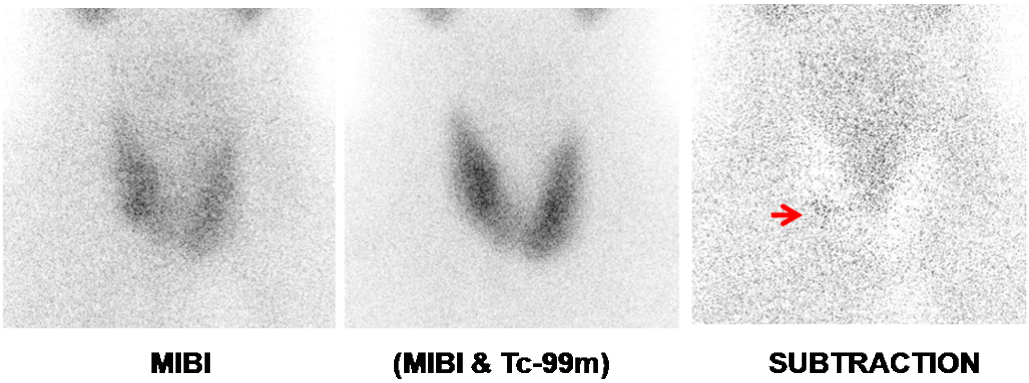

FIGURE 6. DDS performed in patient 3 shows a small focus of selective MIBI uptake projected on the lower pole of the right lobe consistent with small HFPG (red arrow).

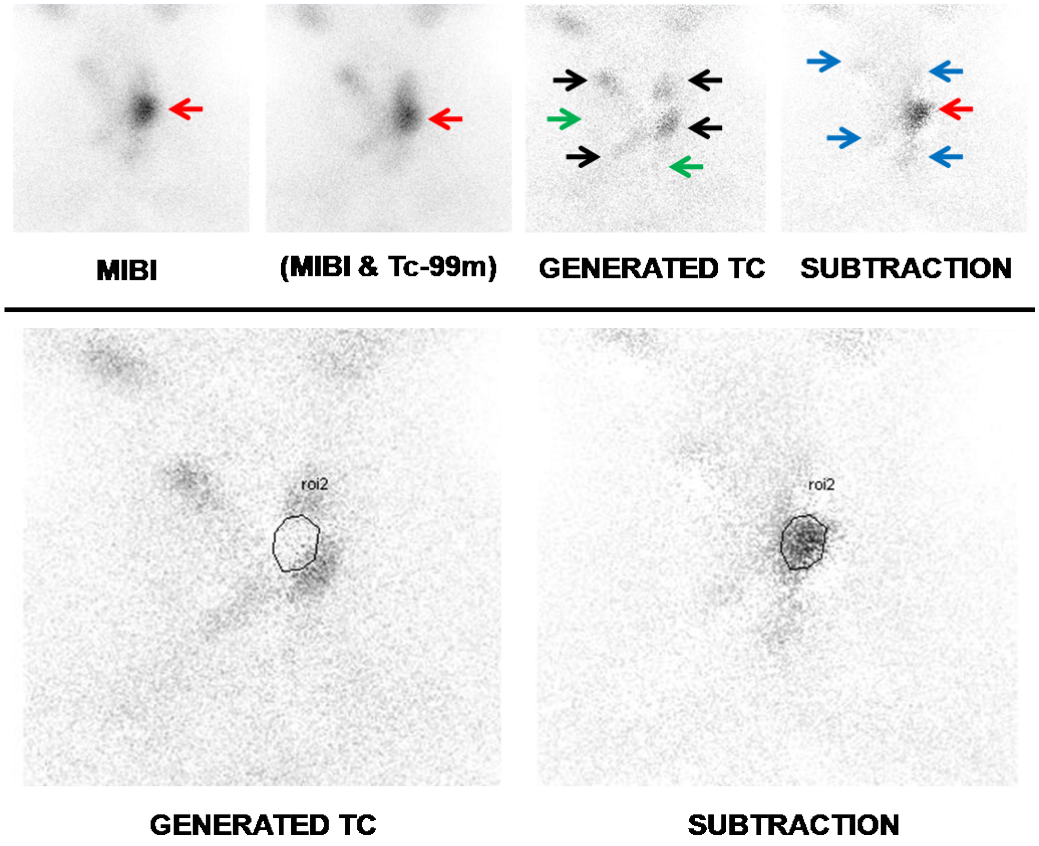

FIGURE 7. Illustrates the DDS realized in patient 4 is representative of primary HPT with concomitant toxic multi-hetero-nodular thyroid goiter. Subtraction parathyroid image shows a hot spot of TP MIBI uptake, projected on the left middle lobe (red arrow) and consistent with intrathyroidal parathyroid adenoma. The generated TC thyroid image reveals bilaterally at least 6 nodules, being 2 cold (green arrows) and 4 functionally active (black arrows). It is difficult to discern on the subtraction image, between the parathyroid adenoma (red arrow) and the thyroid nodules (blue arrows). The ROI drawn for the parathyroid adenoma located in the left lobe is projected in a cold area of the TC thyroid image. Thus, the parathyroid adenoma retains the MIBI only (TP lesion) and has different behavior from the small functional thyroid nodules that retain both tracers (TN lesions).

5. In patient 5, the large field anterior view image of neck/mediastinum, including the parotid glands and myocardium, acquired by the parallel-hole collimator, discloses a tiny focus of activity projected along the upper anterior mediastinum **(FIGURE 8A).** Using the pinhole collimator, the TP ectopic lesion is better visualized, as it is focused and magnified. A supplement enhanced CT was performed to refine the anatomic location of this lesion afterwards.

6. In uremic patient 6, the DDS showed 3 foci of moderate selective tracer uptake, interpreted as 3 TP lesions; 1 focus is projected at the left lower lobe and 2 along the right medial upper and middle lobe **(FIGURE 9).** This case demonstrates the good performance of the DDS protocol in patients with multiple HFPG.

▪ Surgery and histopathology

Results of the on-site open readings of our DDS scintigraphy were used by surgeons to plan and perform surgical interventions. Surgeons also used data from the supplement ECHO and CT. Abnormal parathyroid glands were removed, commonly 1 adenoma in the 5 patients with primary HPT, and 3 hyperplastic glands in the patient with secondary HPT. Three patients with single orthotopic HFPG (patients 1, 2 and 3) underwent minimally invasive surgery. Total thyroidectomy with parathyroidectomy was performed in the patient with primary HPT and concomitant toxic nodular thyroid goiter (patient 4). A thoracoscopic parathyroidectomy was adopted in a patient with mediastinal ectopic HFPG (patient 5). In the secondary hyperparathyroidism case with 3 HFPG revealed by the DDS (patient 6), exploratory surgery was realized in order to excise the 3 parathyroid lesions. Histological analysis of frozen sections was used to confirm the presence of parathyroid tissue. The definitive histopathological examination was gathered as a gold standard to analyze the results of our protocol of nuclear imaging. **TABLE 1** summarizes the biological, histological, and imaging findings of our 6 selected cases of HPT. In our cases of primary HPT, there was a tendency of linear correlation

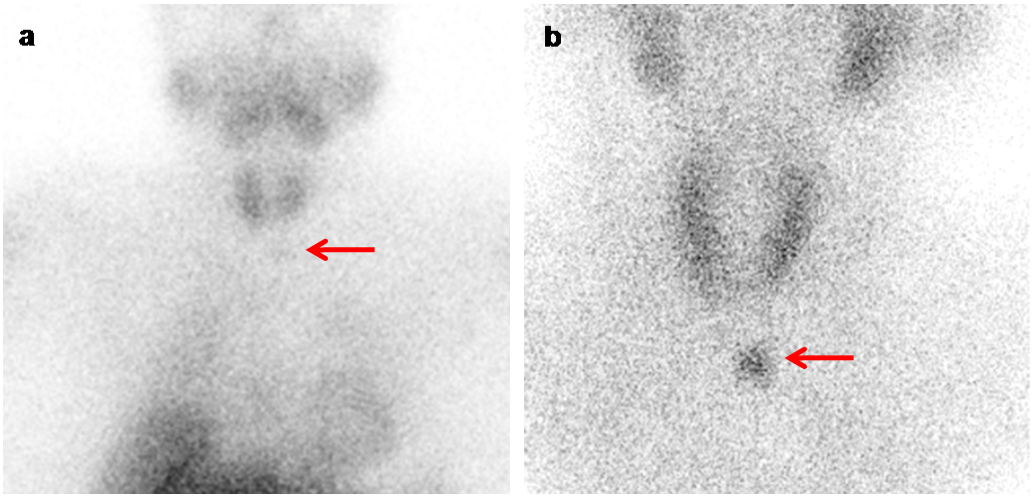

FIGURE 8. Highlights the importance to use the pinhole collimator. The large field anterior view of the MIBI image of neck/mediastinum (a), acquired by the parallel holes collimator in patient 5, depicts a tiny focus of activity projected along the upper anterior mediastinum; this focus is magnified and better visualized using the pinhole collimator (b), which consists with an ectopic parathyroid adenoma (red arrows).

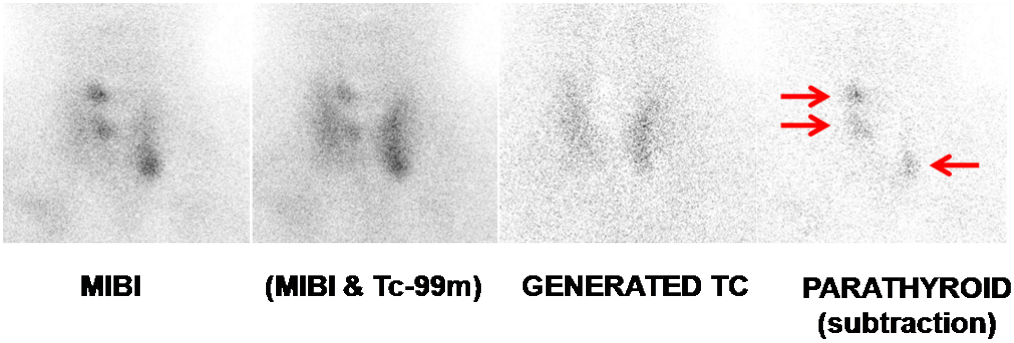

FIGURE 9. Represents the DDS performed in patient 6 with secondary HPT; the subtraction image detects and localizes 3 HFPG, which are projected 1 along the left lower lobe, and 2 along the right medial upper and middle lobe of the thyroid (red arrows); the generated TC (thyroid) image shows no pattern of nodular formation or any source of FP result.

TABLE 1.Summarizes the biological, histological, and imaging findings of our 6 selected cases of HPT.

Patients	HPT	PTH ng/L	Ca mg/dl	Histology	Scintigraphy	Conventional imaging
1	Primary	153	10.9	1 adenoma: 0.8 g	1 TP lesion of high activity	Echo: 1 TP lesion
2	Primary	132	11.1	1 adenoma: 0.9 g	1 TP lesion of moderate activity 1 TN lesion as artifact	Echo: 1 TP lesion
3	Primary	87	10.7	1 adenoma: 0.3 g	1 TP lesion of mild activity	Echo: 0 TP lesion
4	Primary Nodular goiter	180	11.5	1 adenoma: 1.2 g	1 TP lesion of high activity 3 TN lesions as thyroid nodules	Echo: 0 TP lesion
5	Primary	164	11.3	1 adenoma: 1.3g	1 TP ectopic lesion of high activity	CT: 1 TP lesion Mediastinal mass
6	Secondary	271	11.9	3 hyperplastic glands: 0.9g, 0.7g and 0.5g	3 TP lesions of moderate activity	Echo: 1 TP lesion

***Note:** TP: True positive. TN: True negative. Echo: Echography.

between the activity level of the TP foci, the size of HFPG documented by histology, and the PTH and Ca+ serum levels. In the secondary HPT case, the existence of multiple HFPG of moderate activity cumulated the manifestly elevated serum levels of PTH and Ca+.

Discussion

The different radiotracers used in PTS are non-specific and were initially introduced for isotopic imaging of myocardium, as the Tl-201, the MIBI, and the Tc-99m-tetrofosmin (TFSM). They are taken up by both the HFPG and the thyroid parenchyma. In conjunction, the Tc-99m, I-123, or I-131 could be used in order to map the thyroid gland parenchyma and perform a dual-tracer pair images visual comparison or image subtraction [10]. In general, the

approximate cost of the administered activity of I123 by a patient is 2 times more expensive than the cost of the Tl-201 or I-131, 10 times of the MIBI or TFSM, and 20 times of the Tc-99m. Our dual-tracers MIBI/Tc-99m double subtraction protocol is one of the cheapest nuclear techniques using Tc-99m traceable vectors. The dual-tracers Tl-201/Tc-99m subtraction PTS is the oldest protocol being practiced in the 1980s [11]. The long half-life of Tl-201, which is 3 days, exposes the patients to an effective dose that is 3 times higher than that of the Tc-99m labelling vectors [12]. The incidental take-up of MIBI by HFPG was described in 1989 [13], a radiopharmaceutical that becomes the reference in the radionuclides imaging of HPT nowadays. It is a lipophilic molecule that crosses the cell membranes and intracellularly accumulates in the mitochondria [14-16]. Since the 1990s, the MIBI replaced the Tl-201 because of its superior image quality, more favorable dosimetry, and improved detection sensitivity. Several variants of PTS, at least18 based on MIBI, have been used by the nuclear medicine community in planar or tomographic acquisition modes [17]. They can be described under two main methodologies, the single-tracer (MIBI or TFSM) dual-phase imaging and the dual-tracer (Tc-99m/MIBI or I-123/MIBI) subtraction imaging. Until now, there is no established uniform protocol of MIBI PTS, and at close performances, some protocols can be restrictive due to their high cost and/or relatively long execution time. The single tracer dual-phase (early and delayed phases) PTS was suggested by Taillefer et al. Based on the observation that MIBI washes out more rapidly from the thyroid gland than from HFPG. The neck is imaged 5 min, and at 2 to 3 h after MIBI administration. The "differential washout" phenomenon improves target-to-background activity, revealing a selective tracer uptake on the delayed phase by HFPG that should become more visible. The idea in practicing the dual-phase technique is "pleasantly simplistic"; when a single radiopharmaceutical is used, only 2 early and delayed planar static images are acquired, a large field anterior view of neck/mediastinum is recorded, and a parallel holes collimator is used. However, the disadvantages of this technique are numerous. The dual-phase requires a long time of ppT of at least 4 h in the nuclear medicine facility, it has moderate sensitivity, and cannot identify cases of multiple HFPG most of the time [18-20]. Moreover, it may lead to pitfalls results. A False-Negative (FN) detection occurred in HFPG that is characterized by rapid leaching of MIBI [21], whereas the coexistent nodular goiter and autoimmune diseases of the thyroid were responsible for False-Positive (FP) results by enhancement and prolonged retention of MIBI [22]. Thus, subtraction imaging techniques are helpful since not all parathyroid lesions retain MIBI for a long duration, and not all thyroid lesions wash it out quickly.

In contrast with the majority of dual-tracer subtraction protocols described in the literature, which indicate injecting the Tc-99m first before the MIBI, with our protocol the MIBI is injected first [23]. Our method avoids the background noise of the prior injected Tc-99m and allows acquiring under different views the g ood quality MIBI images of HFPG, being either in orthotopic or ectopic positions **(FIGURES 2 and 8).** Several teams advocating the Tc-99m injection first were urged to mediate an oral perchlorate medication that accelerates its washout from the thyroid parenchyma. This intervention improves the quality of the MIBI images acquired after the Tc-99m thyroid image and facilitates the individualization of the HFPG, particularly those located behind the thyroid gland [24]. Other teams, adopting the dual-phase protocol, perform at the 2nd or 3rd h a Tc-99m thyroid image. In both techniques of injecting the Tc-99m before the MIBI or at 2 to 3 h later, the correction of the second tracer image for residual first tracer activity as well as the subtraction of images that are acquired in different g eometric c onditions a re c omplicated and often produces artifacts. Therefore, it is preferable in these techniques to assess the parathyroid abnormalities by visual comparison of the pair Tc-99m and MIBI images.

The pinhole collimator acquisition is adopted in our protocol to obtain magnified images of the thyroid region, improving both the spatial resolution and the detection of the HFPG [25,26]. The left and right lateral views of the cervical region are parts of our scintigraphic protocol allowing the in-depth visualization of HFPG, which are often located behind the upper and lower poles of the thyroid gland **(FIGURE 2).** The prevalence of ectopic HFPG is up to 16% and 14% in patients with primary and secondary hyperparathyroidism, respectively. The lateral views can help to detect some superior ectopic lesions that are not visualized on the anterior view but possibly located in the tracheoesophageal groove and retro esophageal region. Inferior ectopic parathyroid lesions are most frequently found in the anterior mediastinum, in association with the thymus or the thyroid gland [27]. The large field anterior view image of neck/mediastinum, including parotid glands and myocardium, is mandatory and should be

part of any PTS protocol to exclude the ectopic HFPG. In patient 5, this acquisition has allowed disclosing the tiny focus of activity projected along the upper anterior mediastinum consistent with ectopic parathyroid adenoma **(FIGURE 8).** This focus was better visualized using the pinhole collimator, providing a magnified image. The precise anatomic location of ectopic lesions must be documented using enhanced cross-sectional imaging of CT or MRI.

Some nuclear medicine teams, adopting the single-tracer MIBI dual-phase protocol, follow the planar imaging by single-photon emission computed tomography (SPECT) acquisition to enhance the contrast and increase the sensitivity of detection of HFPG. Other teams using hybrid machines propose the simultaneous combination of the SPECT functional images and the CT anatomical images to elucidate the exact volumetric location of the HFPG. The latter strategic method provides highly valuable data before minimally invasive parathyroidectomy. A large meta-analysis was conducted on prospective and retrospective studies concerning these methodologies using a single MIBI tracer. It has concluded that combined SPECT/CT data was by far more sensitive and accurate than the planar mode or the SPECT mode alone. The SPECT and the planar modes had a similar limitation in the diagnostic efficacy, regarding the limited degree of providing anatomic details [28].

Even though pinhole and SPECT/CT acquisitions improve the sensitivity of the single tracer MIBI PTS, the percentage of detected cases of multiple HFPG remains limited. According to continuing education paper, single-tracer dual-phase scintigraphy cannot reliably guide targeted parathyroid surgery in multiple HFPG. An accurate subtraction protocol using two radiopharmaceuticals traceable by two different radioisotopes, the MIBI, and the I-123, has demonstrated high diagnostic values expressed in terms of sensitivity (SS) and positive predictive value (PPV). It is based on the simultaneous dual I-123/MIBI isotopes acquisition by pinhole planar or SPECT/CT modes [29,30]. As compared to our MIBI/Tc-99m dual tracer protocol, the I-123/MIBI dual isotopes simultaneous image halves the acquisition time of the thyroid region. Moreover, the mandatory motion-less imaging time of the cervical region is markedly reduced with subsequent minimization of the motion artifacts in the subtraction image. The I-123 is intravenously administered 3 to 4 h and the MIBI 5 to 15 min before the commencement of gamma-camera imaging. Therefore, the I-123/MIBI dual-isotopes subtraction protocol requires a long duration, at least 4 hours, of the ppT in the nuclear medicine department. **TABLE 2** summarizes the technical characteristics of the most common scintigraphic protocols of PTS practiced on a worldwide scale. This table includes our DDS protocol, which is the shortest in terms of ppT in the nuclear medicine department. The goT of all these protocols is nearly identical, not exceeding 60 min.

In the dual tracer subtraction techniques, the use of Tc-99m instead of I-123 precludes the simultaneous images acquisition of the HFPG and thyroid gland, and the subsequent image

TABLE 2.Compares the technical characteristics of the most common scintigraphic protocols of PTS practiced on a worldwide scale; it includes our dedicated protocol.

Protocols	Tracers	Acquisition	Collimator	goT Per Image	goT Total	ppT
Dual-phase	Single tracer: MIBI	Neck/mediastinum Additional neck	Parallel-hole Pinhole	2 × 5 min 2 × 10 min	30 min	3 h
Dual-phase	Single tracer: MIBI	Neck/mediastinum Additional SPECT/CT	Parallel-hole Parallel-hole	2 × 5 min 1 × 20 min	30 min	3h
Subtraction with perchlorate intervention	Dual tracer : Tc-99m MIBI MIBI	 Neck/mediastinum Neck/mediastinum Additional delay	 Parallel-hole Parallel-hole Parallel-hole	 1 × 5 min 7 × 5 min 1 × 5 min	45 min	3 h
Subtraction DDS protocol	Dual tracer : MIBI MIBI MIBI (MIBI&Tc-99m)	 Neck/mediastinum Neck lateral views Neck ant view Neck ant view	 Parallel-hole Pinhole Pinhole Pinhole	 1 × 5 min 2 × 5 min 1 × 10 min 1 × 10 min	45 min additional 10 min waiting after second tracer injection	1 h
Subtraction	Dual isotope: I-123/MIBI I-123/MIBI I-123/MIBI	Simultaneous Neck Neck/mediastinum Additional SPECT/CT	 Pinhole Parallel-hole Parallel-hole	 10 min 10 min 20 min	40 min	4 h

***Note:** ppT = Patient presence time in nuclear medicine facility; goT = Gamma camera occupation time; DDS: Dual tracer double image subtractions protocol.

subtraction may suffer from motion artifacts, which are the source of FP results. In patient 2, the motion artifact revealed on DDS images was easily recognized along the edge of the thyroid gland **(FIGURE 5)** and considered as TN. It was related to the non-exact superimposition of MIBI and (MIBI&Tc-99m) planar images. We think that motion of head/neck occurring with any technique of parathyroid scintigraphy, even with I-123/MIBI dual isotopes simultaneous acquisition, can cause FN findings due to the dispersion of the activity of a true lesion in a large area of the resulting image becoming subsequently non-detectable. Therefore, an adapted immobilization device fixing the head/neck during the successive image acquisitions can avoid the motion artifacts. Another kind of artifacts was found in 3.4% of cases of I-123/MIBI dual isotopes simultaneous acquisition when subtraction concerns the volumetric SPECT/CT images. They are independent of patient motion, named edge artifacts, and half of them can be correctly classified as TN with additional pinhole imaging. This phenomenon can be reduced by the implementation of adapted collimation as well as adequate parameters of acquisition, processing, and scatter/cross-contamination correction [31].

MIBI avid thyroid nodules are not well discriminated from the HFPG using the additional Tc-99m tracer, and multi-nodular goiter is well known to be a source of FP in PTS [32]. On the contrary, the simultaneous acquisition of the I-123 image allows the specific identification of cold or hot thyroid nodules as well as residual thyroid tissue, avoiding the pitfalls resulting from the MIBI image. In this setting, although the nuclear medicine physician is well experienced, reading of MIBI and Tc-99m images of the dual tracer protocols are challenging, acquired either on planar or SPECT/CT mode. In our case of DDS performed on patients with multi-nodular thyroid goiter (patient 4), discernment of the TP active focus of parathyroid adenoma from the TN foci related to thyroid nodules was difficult. We should have drawn an ROI to demonstrate the different behavior of the parathyroid adenoma retaining the MIBI only, and the thyroid nodules retaining both MIBI and Tc-99m tracers.

In our 6 selected cases of primary and secondary HPT, the DDS protocol allows recognition of both TP and TN lesions of HFPG, a fact that may reflect high performances. The TP lesions were recognized as well in all patients and the TN lesions in cases of motion artifact (patient 2) and multi-hetero-nodular thyroid goiter (patient 4).High performances of DDS, as a good SS, is especially remarkable in the 2 cases of single small parathyroid adenoma and multiple hyperplastic parathyroid glands (patients 3 and 6, respectively). They indicate the potential role that can be played by our protocol in parathyroid imaging. A large representative sample, preferably multi-centric, is required as a confirmation of these single-institution results. A retrospective pilot study of the DDS protocol is underway, enrolling more than 250 cases of primary and secondary hyperparathyroidism.

Besides the technical factors discussed above, there are histological and biochemical factors that affect the SS of the PTS. Significant correlations have been reported between the MIBI uptake and the preoperative PTH and Ca serum levels [33,34]. One of the main factors influencing the scintigraphic localization of HFPG seems to be its size. There is a significant correlation between the MIBI uptake level and the presence of more significant numbers of oxyphil cells reach in mitochondria in both parathyroid adenoma and hyperplastic glands [35]. Biological, histological, and scintigraphic results observed in our cases of HPT are in concordance with the literature data. In the 6 patients with primary and secondary HPT, there was a tendency of linear correlation between the activity level of the TP foci, the size of HFPG, and the corresponding PTH and Ca serum levels.

Conclusion

At present, among the numerous scintigraphic protocols described in the literature, the dual-isotope I-123/MIBI subtraction scintigraphy with the 2 mandatory pinhole and SPECT/CT simultaneous acquisitions has the highest technical performances in patients with single or multiple HFPG. In non-industrial countries, the availability of I-123 often lacks for commercial or economic logistic reasons. Moreover, the daily schedule of nuclear medicine exams is usually loaded into facilities that are equipped with no more than one basic gamma camera. In these conditions, the implementation of cheap and short execution time PTS as our challenging DDS technique of promising reliability can be a good alternative represented by:

1. Use of radiopharmaceuticals traceable by the Tc-99m, a radioisotope daily available in the nuclear medicine facilities fitted with a basic gamma-camera equipped with pinhole and parallel-hole collimators.
2. Easy to execute serial steps of 2

radiopharmaceutical injections and 5 image acquisitions, with simple processing of digital image subtraction.

3. Short execution time, which is expressed in terms of the ppT in the nuclear medicine facility and the goT.
4. Good preliminary performances demonstrated in representative cases; obviously, a confirmation of these single-institution results is required on a larger sample, preferably multi-centric studies.
5. A methodology much cheaper than other techniques requiring the use of expensive radioisotopes of iodine or hybrid SPECT/CT machinery.

References

1. Callender GG, Udelsman R. Surgery for primary hyperparathyroidism. *Cancer*. 120(23), 3602-3616 (2014).
2. Walsh NJ, Sullivan BT, Duke WS, Terris DJ. Routine bilateral neck exploration and four-gland dissection remains unnecessary in modern parathyroid surgery. *Laryngoscope. Investig. Otolaryngol*. 4(1), 188-192 (2018).
3. Wojtczak B, Syrycka J, Kaliszewski K *et al*. Surgical implications of recent modalities for parathyroid imaging. *Gland. Surg*. 9(2), S86-S94 (2020).
4. Liddy S, Worsley D, Torreggiani W, Fenney J. Preoperative imaging in primary hyperparathyroidism: literature review and recommendations. *Can. Assoc. Radiol. J*. 68(1), 47-55 (2017).
5. Hindié E, Zanotti-Fregonara P, Tabarin A *et al*. The role of radionuclide imaging in the surgical management of primary hyperparathyroidism. *J. Nucl. Med*. 56(5), 737-744 (2015).
6. Moralidis E. Radionuclide parathyroid imaging: a concise, updated review. *Hell. J. Nucl. Med*. 16(2), 125-133 (2013).
7. Suehiro M, Fukuchi M. Localization of hyperfunctioning parathyroid glands by means of thallium-201 and iodine-131 subtraction scintigraphy in patients with primary and secondary hyperparathyroidism. *Ann. Nucl. Med*. 6(3), 185-190 (1992).
8. OECD/NEA. The Supply of Medical Isotopes: An Economic Diagnosis and Possible Solutions, OECD Publishing, Paris, (2019).
9. Chehade F, Droubi N, Ramadan G *et al*. Parathyroid scintigraphy with double subtractions images. *Eur. J. Nucl. Med*. 28(8), (2001).
10. Hindié E, Ugur O, Fuster D *et al*. EANM parathyroid guidelines. *Eur. J. Nucl. Med. Mol. Imaging*. 36, 1201–1216 (2009).
11. Winzelberg GG, Hydovitz JD. Radionuclide imaging of parathyroid tumors: historical perspectives and newer techniques. *Semin. Nucl. Med*. 15(2), 161-170 (1985).
12. Xie T, Lee C, Bolch WE, Zaidi H. Assessment of radiation dose in nuclear cardiovascular imaging using realistic computational models. *Med. Phys*. 42(6), 2955-2966 (2015).
13. Coakley AJ, Kettle AG, Wells CP, O'Doherty MJ, Collins RE. 99Tcm sestamibi--a new agent for parathyroid imaging. *Nucl. Med. Commun*. 10(11), 791-4 (1989).
14. Hetrakul N, Civelek AC, Stagg CA, Udelsman R. In vitro accumulation of technetium-99m-sestamibi in human parathyroid mitochondria. *Surgery*. 130(6), 1011-1018 (2001).
15. Cordes M, Dworak O, Papadopoulos T, Coerper S, Kuwert T. MIBI scintigraphy of parathyroid adenomas: correlation with biochemical and histological markers. *Endocr. Res*. 43(3), 141-148 (2018).
16. Taillefer R, Boucher Y, Potvin C, Lambert R. Detection and localization of parathyroid adenomas in patients with hyperparathyroidism using a single radionuclide imaging procedure with technetium-99m-sestamibi (double-phase study). *J Nucl Med*. 33(10), 1801-1807 (1992).
17. Tunninen V, Kauppinen T, Eskola H, Koskinen MO. Parathyroid scintigraphy protocols in Finland in 2010. Results of the query and current status. *Nuklearmedizin*. 49(5), 187-194 (2010).
18. Wei WJ, Shen CT, Song HJ, Qiu ZL, Luo QY. Comparison of SPET/CT, SPET and planar imaging using 99mTc-MIBI as independent techniques to support minimally invasive parathyroidectomy in primary hyperparathyroidism: A meta-analysis. *Hell. J. Nucl. Med*. 18(2), 127-35 (2015).
19. Hindié E, Mellière D, Jeanguillaume C *et al*. Parathyroid imaging using simultaneous double-window recording of technetium-99m-sestamibi and iodine-123. *J. Nucl. Med*. 39(6), 1100-1105 (1998).
20. Caldarella C, Treglia G, Pontecorvi A, Giordano A. Diagnostic performance of planar scintigraphy using ^{99}mTc-MIBI in patients with secondary hyperparathyroidism: a meta-analysis. *Ann. Nucl. Med*. 26(10), 794-803 (2012).
21. Bénard F, Lefebvre B, Beuvon F, Langlois MF, Bisson G. Rapid washout of technetium-99m-MIBI from a large parathyroid adenoma. *J. Nucl. Med*. 36(2), 241-243 (1995).
22. Shafiei B, Hoseinzadeh S, Fotouhi F *et al*. Preoperative ^{99}mTc-sestamibi scintigraphy in patients with primary hyperparathyroidism and concomitant nodular goiter: comparison of SPECT-CT, SPECT, and planar imaging. *Nucl. Med. Commun*. 33(10), 1070-1076 (2012).
23. Taieb D, Urena-Torres P, Zanotti-Fregonara P *et al*. Parathyroid scintigraphy in renal hyperparathyroidism: The added diagnostic value of SPECT and SPECT/CT. *Clin. Nucl. Med*. 38(8), 630-635 (2013).
24. Rubello D, Saladini G, Casara D *et al*. Parathyroid imaging with pertechnetate plus perchlorate/MIBI subtraction scintigraphy: a fast and effective technique. *Clin. Nucl. Med*. 25(7), 527-531 (2000).
25. Serrano Vicente J, Rayo Madrid JI, Luengo Pérez LM, Díaz Pérez de Madrid J. 99m-Tc sestamibi scintigraphy in primary hyperparathyroidism. Importance of lateral projections using a pin-hole collimator. *Rev. Esp. Med. Nucl*. 22(6), 403-409 (2003).
26. Klingensmith WC, Koo PJ, Summerlin A *et al*. Parathyroid imaging: the importance of pinhole collimation with both single- and dual-tracer acquisition. *J Nucl Med Technol*. 41(2), 99-104 (2013).
27. Noussios G, Anagnostis P, Natsis K. Ectopic parathyroid glands and their anatomical, clinical and surgical implications. *Exp. Clin. Endocrinol. Diabetes*. 120(10), 604-10 (2012).
28. Kannan S, Milas M, Neumann D *et al*. Parathyroid nuclear scan. A focused review on the technical and biological factors affecting its outcome. *Clin. Cases. Miner. Bone. Metab*. 11(1), 25-30 (2014).
29. Caveny S, Klingensmith W, Martin W *et al*. Parathyroid imaging: The importance of dual-radiopharmaceutical simultaneous acquisition with 99mTc-sestamibi and 123I. *J. Nucl. Med. Technol*. 40 (2), 104-110 (2012).
30. Ryhänen E, Schildt J, Heiskanen I *et al*. 99mTechnetium sestamibi-123iodine scintigraphy is more accurate than 99mtechnetium sestamibi alone before surgery for primary hyperparathyroidism. *Int. J. Mol. Imaging*. (2015).
31. Tunninen V, Varjo P, Kauppinen T *et al*. 99mTc-sestamibi/123I subtraction SPECT/CT in parathyroid scintigraphy: Is additional pinhole imaging useful? *Int. J. Mol. Imaging*. 1-8, (2017).
32. Torregrosa JV, Félez I, Fuster D. Usefulness of imaging techniques in secondary hyperparathyroidism. *Nefrologia*. 30(2), 158-67 (2010).
33. Khorasani N, Mohammadi A. Effective factors on the sensitivity of preoperative sestamibi scanning for primary hyperparathyroidism. *Int. J. Clin. Exp. Med*. 7(9), 2639–2644 (2014).
34. Parikshak M, Castillo ED, Conrad MF, Talpos GB. Impact of hypercalcemia and parathyroid hormone level on the sensitivity of preoperative sestamibi scanning for primary hyperparathyroidism. *Am. Surg*. 69(5), 393-398 (2003).
35. Nishida H, Ishibashi M, Hiromatsu Y *et al*. Comparison of histological findings and parathyroid scintigraphy in hemodialysis patients with secondary hyperparathyroid glands. *Endocr. J*. 52(2), 223-228 (2005).